Solitonic structures in a nonlinear model with interparticle anharmonic interaction

Maximo A. Agüero and Mauricio J. Paulin
Facultad de Ciencias, Universidad Autónoma del Estado de México, Instituto Literario 100, Toluca 50000, Edo. Mexico, Mexico
(Received 29 March 2000; revised manuscript received 22 September 2000; published 23 March 2001)

Using a special combination of relevant parameters for a model with interparticle anharmonic interactions, we can predict the appearance of solitonic structures. The most remarkable representatives of the structures found here are the so-called drop compactons, (solitons with compact support in the shape of hard spheres), cusps, peak solitons (peakons), and defects. These analytic solutions (similar to others in their family) are obtained by considering strong restrictions on the possible values of their velocities. We analyze two types of physical boundary condition: the trivial and the so-called condensate boundary conditions. The total energy concentrated in each soliton pattern is also calculated.

DOI: 10.1103/PhysRevE.63.046606 PACS number(s): 41.20.Jb

I. INTRODUCTION

Growing interest has been focused on finding exact traveling wave solutions of nonintegrable systems. The various versions of the so-called Frenkel-Kontorova model have been studied and solutions with direct applications in a wide variety of fields obtained. The most remarkable models of this type are the sine-Gordon and Φ^4 systems; see, for example, [1–4] and citations therein. There is clear evidence that kink internal modes are not only limited to the case of a harmonic interparticle interaction; rather, it was found that such solutions also occur in discrete chains, i.e., anharmonic nearest-neighbor interparticle interaction [5–7]. It has also been shown recently that nonlinear lattices can support solitons and other kinds of excitation which behave like shock waves in integrable and nonintegrable lattices [8]. The inclusion of anharmonicity in the study of lattice models can produce a variety of features. For instance, in [9] this inclusion was done by taking into account the interaction between spins and phonons in the quantum Heisenberg model of ferromagnetism. By using the generalized coherent state approach it was possible to find a cubic-quintic nonlinear Schrödinger equation that in a particular case of parametric domain values produces bright, dark, and singular solitons [9–11].

The research involved in finding analytic expressions for soliton structures is stimulated by physical applications and by the interest in fundamental dynamics properties of nonlinear models. Among these, the most interesting structures consist of solutions that resemble ''real'' particles, in the form of hard spheres. These structures, for obvious reasons, will interact with each other only when they come into contact in a way similar to the contact of hard spheres. It is worthy of mention that Rosenau and Hyman [12] found solutions of the solitary type without infinite tails, termed solitons with compact support or compactons. Recently, in the very interesting work [13], the generalized Φ^4 or double well model with anharmonic interparticle interaction in the continuum limit was studied, and various types of kink compacton were found. The analysis was done for specific parameter values that additionally determined the compacton velocities. So at least two questions can be posed at this stage of research. The first is concerned with the possibility of obtaining other types of analytic solitonlike structure for the nonlinear evolution equation (1) below by taking into consideration trivial and condensate types of boundary conditions. The second question concerns the parameter domains where these soliton structures exist.

The purpose of the present paper is to try to answer the questions posed above and discuss the possibility of determining the velocity values of the solitons. Below, we report these findings for the same model proposed in [13]. These strong nonlinear analytic objects were obtained without disregarding nonlinear terms in the equation of motion and considering only different combinations of the main parameters. With this approach the specific velocity values for each soliton pattern were found.

We analyzed this model by considering two types of boundary conditions: the trivial and the condensate types of boundary conditions at infinity as is usual in physics. We will show that for appropriate velocity values the dynamics of the system is dominated by self-sustained traveling solitonic structures. In the case of the trivial boundary condition it was possible to obtain the so-called drop compacton and peak soliton or peakon. It is surprising that it is possible to find such structures by applying the simple reasoning that is common for obtaining other classes of compactons, kink compactons, for example. These solutions are strongly localized in space, they travel without distortions, and they do not present any infinite tails. We use the term drop compacton to designate solutions that in some manner resemble the shape of hard spheres. For the condensate type of boundary condition, we have obtained a rich analytic diversity of soliton patterns that are represented by dark, cusp, peak, kink, and shock structures.

II. THE MODEL AND SOLITONIC STRUCTURES

Let us begin with the equation of motion in the 1+1 space-time manifold proposed in [13]:

$$\Phi_{tt} - C_l \Phi_{xx} + 3C_{nl}\Phi_x^2\Phi_{xx} - 2V_0(\Phi - \Phi^3) = 0. \qquad (1)$$

As usual the subscripts indicate partial derivatives with respect to time t and space x. Equation (1) was obtained as a continuum limit of the equation of motion for a discrete system whose Hamiltonian was proposed as

$$H=\sum_n \left[\frac{1}{2}\left(\frac{d\Phi_n}{dt}\right)^2+\frac{V_0}{2}(1-\Phi_n^2)^2+U(\Phi_{n+1}-\Phi_n)\right] \tag{2}$$

with interaction potential between sites taken as

$$U(\Phi_{n+1}-\Phi_n)=\frac{C_l}{2}(\Phi_{n+1}-\Phi_n)^2+\frac{C_{nl}}{4}(\Phi_{n+1}-\Phi_n)^4. \tag{3}$$

Here Φ_n denotes the position of the nth particle measured from the nth lattice site, V_0 and C_l are constant parameters, and C_{nl} is the parameter that controls the strength of the nonlinear coupling.

As was mentioned above, Eq. (1) has been treated analytically for several important cases [13] and kink compactons were obtained, that is, solitonic kinks with compact support. Indeed, in subsequent papers their properties and other solutions were analyzed in great detail [14,15]. The velocities of the kink compactons were determined from the relation $u^2-C_l=0$. In our treatment we will not consider this relation because its use could imply energy divergence for our localized structures. We now analyze the same equation (1) and try to find the velocity values for existing solitonic patterns. In order to do this we begin with a primary constriction: the essential features of physically available solutions are determined by imposing the boundary condition. Let us first analyze the case of the drop type of boundary condition.

A. Drop type of boundary condition

Now, for Eq. (1) we take into consideration the independent variable $\zeta=x-ut$ in order to find, as usual, traveling waves $\Phi(\zeta)=\Phi(x-ut)$ with constant velocity u. The trivial or drop boundary condition is determined by the expressions

$$\Phi\to 0,\quad \Phi_\zeta\to 0 \quad \text{at}\ \ \zeta\to\pm\infty, \tag{4}$$

One can simplify Eq. (1) using the relations (4) and considering

$$\Phi_t=-u\Phi_\zeta,\quad \Phi_x=\Phi_\zeta,$$

and after integrating one has

$$(\Phi_\zeta)^4-F(\Phi_\zeta)^2+G\left(\frac{\Phi^4}{2}-\Phi^2\right)=0. \tag{5}$$

Here $F=2(C_l-u^2)/3C_{nl}$ and $G=4V_0/3C_{nl}$. In order to solve the differential equation (5), it seems natural to introduce the following ansatz. Solitonlike structures are available if the parameters of the strong model satisfy the following relation:

$$(u^2-C_l)^2+6V_0C_{nl}=0. \tag{6}$$

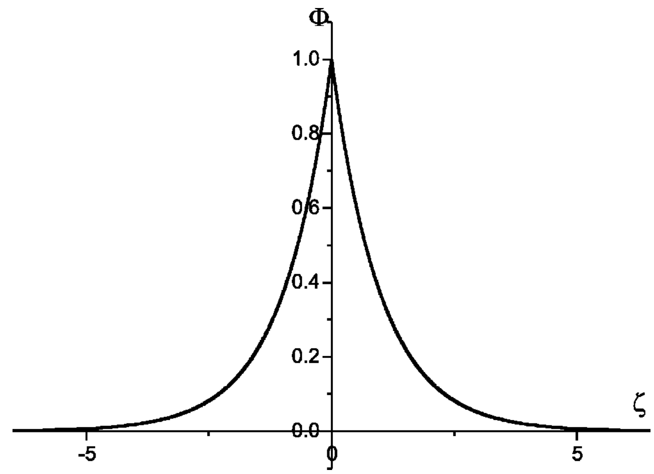

FIG. 1. Peaklike soliton that is obtained by merging two parts of the solution (7). With increasing F, the peak becomes more acute.

After some algebra the solutions can be found analytically and, for the sake of clarity, let us classify them in the following manner.

(a) Peak soliton. These solutions emerge when the general equation (5) is transformed using Eq. (6) to

$$\Phi_\zeta=\pm\sqrt{\frac{F}{2}}\Phi.$$

Applying the boundary conditions (4), and solving the above differential equation, it is easy to find the peakon defined by merging the next two solution branches:

$$\Phi(\zeta)=\exp\left(\pm\sqrt{\frac{F}{2}}(\zeta-\zeta_0)\right). \tag{7}$$

The positive sign of the exponential branch corresponds to the case where $\zeta\leqslant\zeta_0$ and the negative one to $\zeta\geqslant\zeta_0$. The graphic that represents this solution is presented in Fig. 1, while the value of ζ_0 is determined naturally by the initial condition. When the values of F increase ($u^2\to C_l$) the peakon shape transforms to the form of a δ function. A similar unusual solitary wave, named a peakon, was found in [16] for a different type of nonlinear evolution equation.

(b) Drop compactons. We introduce this name to designate solutions that usually have the form of hump solitons but are defined now only in a finite space sector, and because of their forms and properties are reminiscent of hard spheres. Outside this sector, the field vanishes. In other words, this is in some manner the common drop soliton but without its infinite tails. The determined equation for obtaining these solutions is

$$\Phi_\zeta=\pm\sqrt{F\left(1-\frac{\Phi^2}{2}\right)}.$$

From here it is easy to find the solutions

$$\Phi=\pm\sqrt{2}\sin\left[\sqrt{\frac{F}{2}}(\zeta+\zeta_0)\right], \tag{8}$$

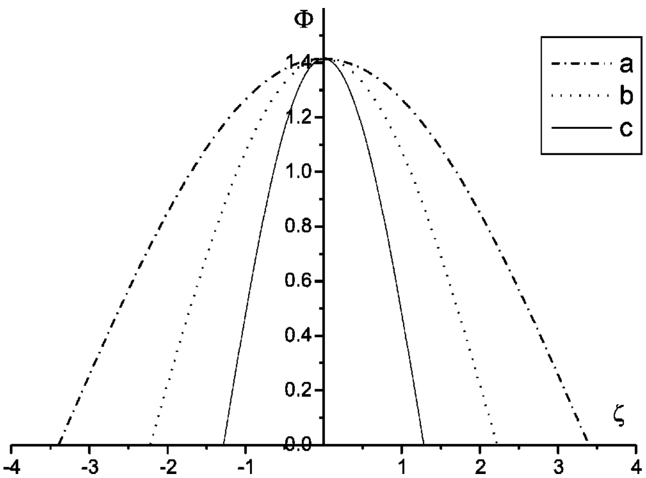

FIG. 2. Drop-compacton solutions. They change their shape in the space ζ while their amplitudes remain constant. Here we present three curves at fixed values $V_0=1/2$ and $u=3$ and varying the parameter C_l: (a) $C_l=2$, (b) $C_l=5$, and (c) $C_l=8$.

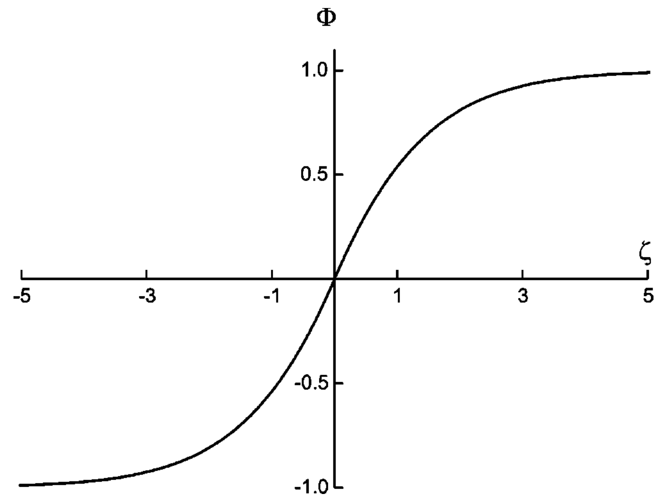

FIG. 3. Typical kinklike structure without small perturbation near its center. This solution corresponds to the configuration (a) for the boundary condition Eq. (17).

where Φ lies between $-\sqrt{2}$ and $\sqrt{2}$ and $F=V_0/(u^2-C_l)$. Because of the restriction imposed by the boundary condition (6), it is reasonable to now make the following statement: solitonic structures can be obtained by choosing the initial condition $\sqrt{F/2}\zeta_0=\pi/2$ that determines the center of mass of the drop (antidrop) compacton when $-\pi/2 \leqslant \sqrt{F/2}\zeta \leqslant \pi/2$. Thus, it appears to be possible to find drop-compacton solutions upon the fulfillment of the above strong requirements. The width of this drop-compacton can be evaluated easily and has the form

$$L=\pi\sqrt{\frac{2}{F}}.$$

When we observe the properties of this structure on considering the variation of its parameters, we find some interesting behavior that leads us to use the name ''drop compacton.'' Indeed, it is easy to check that when $u^2 \to C_l$ and with a fixed value of V_0 in Eq. (6), the ''volume'' of the drop compacton decreases due to the increase of F, while its amplitude remains constant. In the opposite case, when F is decreasing, the velocity does not approach the value of C_l, and the ''volume'' increases. In both of these cases, the third parameter C_{nl} is defined from Eq. (6). As an illustration of this fact we have provided Fig. 2, where three different drop compactons with different lengths or ''volumes'' are shown.

Now, we evaluate the energy of these configurations. We can calculate the total energy localized in the solitonic traveling structures with velocity u by means of the following expression:

$$E^1_{total}=\int_{x_1}^{x_2}\left[\frac{1}{2}\Phi_t^2+\frac{1}{2}C_l\Phi_x^2+\frac{1}{4}C_{nl}\Phi_x^4 + V_0(\Phi^2/2-1)\Phi^2\right]dx, \tag{9}$$

where x_i is determined by the region of existence for each concrete case of solitonic structures. Using the above expression one obtains

$$E_{dc}=\frac{\pi}{2\sqrt{2}}(3C_l+u^2)\sqrt{\frac{V_0}{u^2-C_l}}. \tag{10}$$

From this relation we observe that the energy for traveling compacted drops is limited by their velocity values. Indeed, when $u^2 \to C_l$, the energy (10) tends to be infinite. Consequently, the nonavailable velocities for these solutions are $u_0=\pm\sqrt{C_l}$. It is surprising to notice that these velocity values allow the existence of the kink compactons (let us call them the first type) studied in [13]. From here, one can infer that drop compactons cannot coexist with first type kink compactons since the two types of compacton exist in different regions of the parameters delimited by their velocities. Consequently, this crucial value can be regarded as a point of bifurcation. When the velocities of our traveling solutions approach the value of u_0, kink compactons arise. This system behavior suggests to us the appearance of a phase transition of second order at this point of bifurcation. This is because, outside the value of u_0, the system is in a state that supports drop compactons and peakons, and exactly at the value u_0 kink compactons appear, determining the second state of the system.

Finally, evaluating the energy of the peak solitons, one arrives at the expression

$$E_p=\frac{(11C_l+u^2)}{6\sqrt{2}}\sqrt{\frac{V_0}{u^2-C_l}}. \tag{11}$$

It is easy to see in this case also, that there is a divergent value of energy when this peakon travels with velocity equal to $u_0=\pm\sqrt{C_l}$.

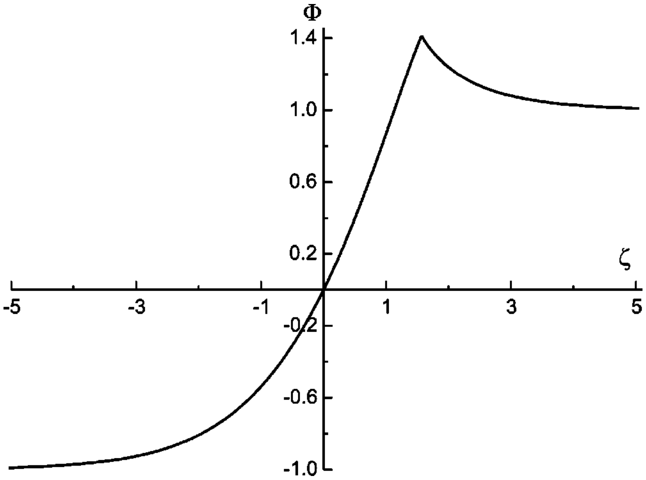

FIG. 4. Kink soliton with small hump near its center that can be treated as a traveling well domain. This is the (b) configuration for the condition (17).

B. Condensate type of boundary condition

Traveling wave solutions $\Phi(\zeta)=\Phi(x-ut)$ with constant velocity u can also be obtained when the boundary conditions are determined by the expressions

$$\Phi\rightarrow\pm 1, \quad \Phi_\zeta\rightarrow 0 \quad \text{at} \quad \zeta\rightarrow\pm\infty. \tag{12}$$

As a result of the application of the boundary condition (12) to Eq. (1) we obtain the nonlinear equation

$$(\Phi_\zeta)^4-A(\Phi_\zeta)^2+B(1-\Phi^2)^2=0, \tag{13}$$

with $A=2(u^2-C_l)/3C_{nl}$, $B=-2V_0/3C_{nl}$, and $C_{nl}\neq 0$. We can now exploit the technique used above for finding drop and peakon solutions, in order to analyze this equation. Skipping the details, we find that the integration of Eq. (13) occurs when the following relation holds:

$$(u^2-C_l)^2+6V_0C_{nl}=0. \tag{14}$$

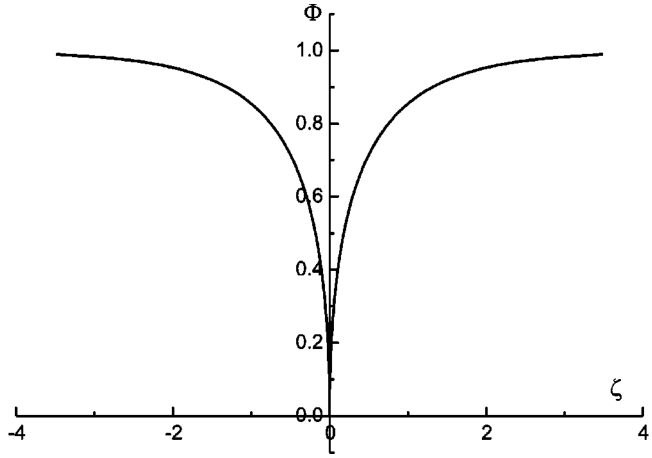

FIG. 6. Cusp soliton in the form of a straight bubble directed down that is an acute dip in the condensate. This figure represents the relations (d) of Eq. (18).

Thus, the signs of V_0 and C_{nl} have to be opposite to each other. We aim to use this powerful restriction to find solitonic structures. Substituting Eq. (14) into Eq. (13) and trying to find solutions that satisfy the condensed type of boundary condition (12), one obtains a set of inverse functions $\Phi(\zeta)^{-1}$ that can be conveniently written as

$$\pm\sqrt{A}(\zeta_{lmn}-\zeta_0)=\arcsin\left(\frac{l\Phi}{\sqrt{2}}\right)+\ln\left[m\sqrt{1-\frac{\Phi^2}{2}}+\frac{n\Phi}{\sqrt{2}}\right], \tag{15}$$

where $l,m,n=+,-$, i.e., these symbols simply indicate the sign of each denoted term in the right-hand side of Eq. (15), and ζ_0 is defined by the chosen initial condition, i.e., when $\zeta=0$.

Let us analyze Eq. (15). It is readily observed that for this case we have four pairs (possibilities) of defined boundary conditions according to the definition (12). Each pair pro-

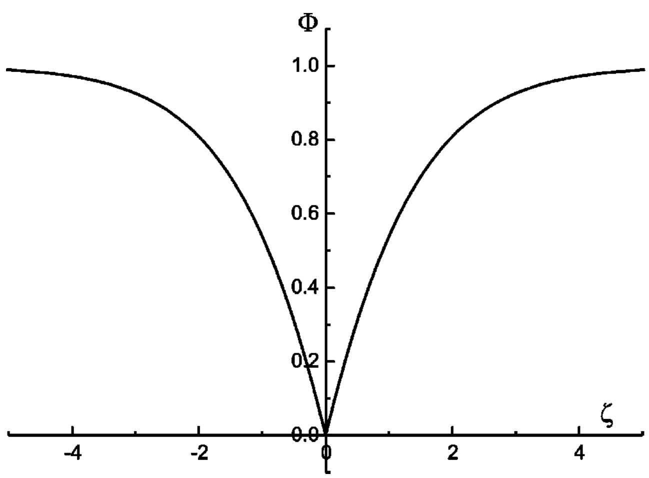

FIG. 5. Solitonic structure that we named the peak bubble because of its rarefied form in the center; representation (c) for the condition (18).

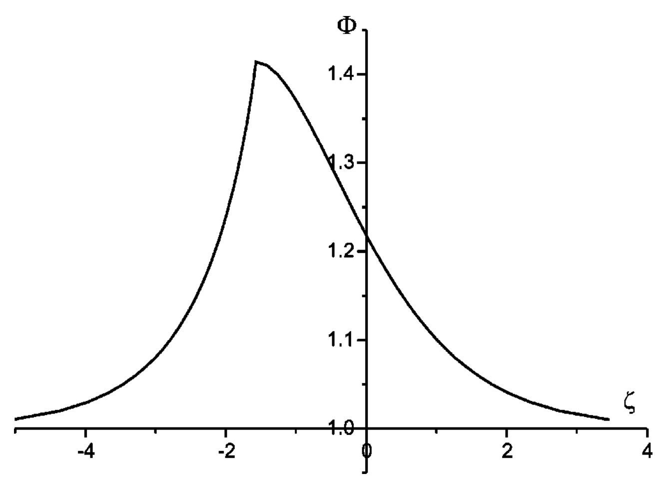

FIG. 7. Solution like a peakon that represents an excitation to the constant condensate. The corresponding conditions are given by (e).

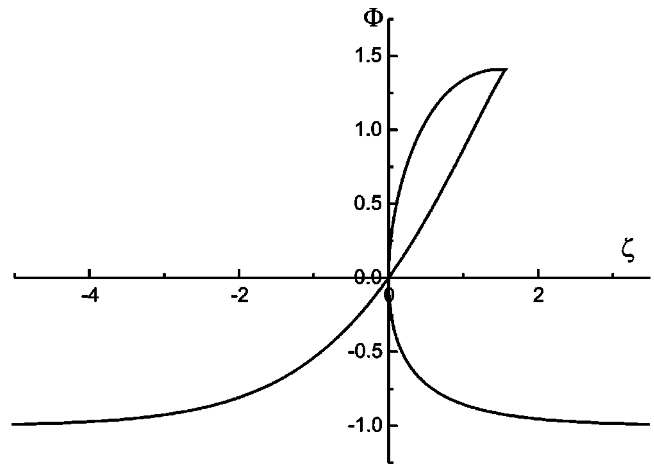

FIG. 8. This is an example of an exotic solution that has the shape of a loop [see relations (f) in text]. Unfortunately, its corresponding energy value is divergent.

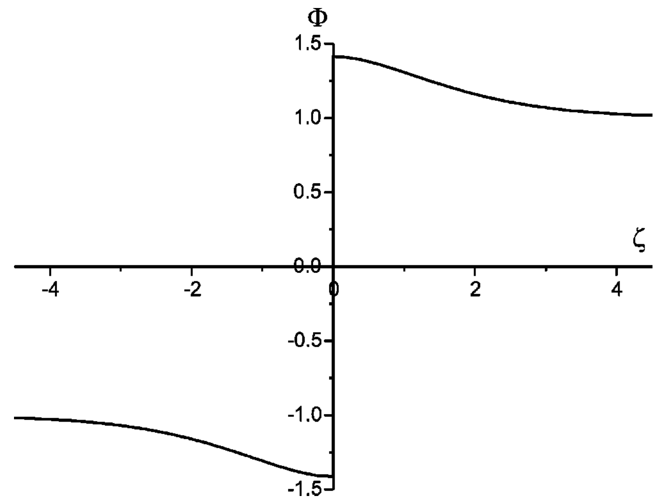

FIG. 10. Second type of shock structure with a form like a domain well that appears provided configuration (h) is satisfied.

duces two branches to construct the solutions. One of them is mainly situated in the negative sector of ζ while the other branch is in the positive one.

In what follows, we make the assumption that at a suitable point ζ_0 in the space ζ the two branches of the solution defined by inverting Eq. (15) merge into each other and one can easily recover the soliton forms. The criteria for determining this point of coalescing depend very much on the initial configuration of the system. This is similar to the procedure of centering the solutions. Such restrictions imply that in some cases we have to ''move'' one of the solutions to the left or to the right for merging. In other cases, such operations are necessary since we will restrict ourselves only to solutions without ambiguities: when the two branches do not show explicit values for a certain region of the independent variable ζ. In this way, in only a few cases is the continuous condition satisfied; usually at the point of merging we have discontinuities. One of the very surprising solutions obtained utilizing this approach is the so-called loop soliton. Since each branch of the solution (for each pair of determined boundary conditions) travels with the same velocity u, the necessary gap Δ in the space ζ for coalescing solutions, determined by the initial conditions, can be presented in two types:

$$\Delta_1 = 0, \quad \Delta_2 = \arcsin[1] = \pi/2. \tag{16}$$

With these statements in mind, we can show below that the inverse function of $\zeta(\Phi)$ of Eq. (15) shows structures that resemble the usual bell, peak, cusp, shock, kink, and bubble types of soliton. Additionally, loop soliton solutions were found. Thus, different velocity restrictions accompanied by the creation of solitonic structures occur when the signs in Eq. (15) are determined by the boundary conditions. We report the best representative configurations in the following.

Let us first take the solutions when they merge in the ''space'' with $\Delta_1 = 0$; thus for

$$\Phi \to -1 \ \text{ while } \ \zeta \to -\infty, \quad \Phi \to 1 \ \text{ while } \ \zeta \to \infty. \tag{17}$$

The solitonic structure can be defined by

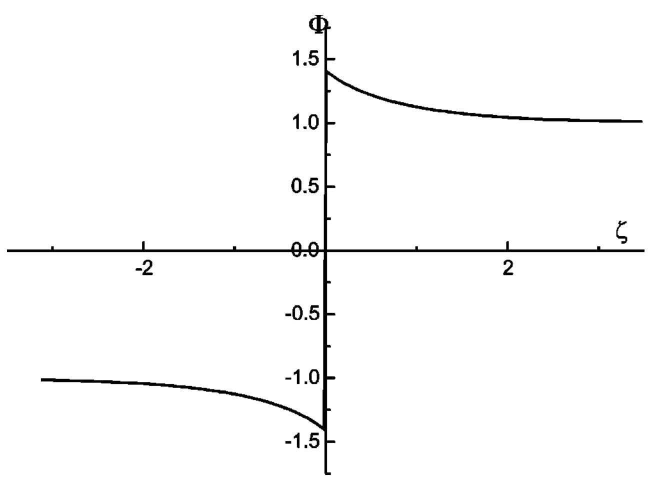

FIG. 9. Typical shock structure that is moving in the medium as a defect and represents the configuration (g).

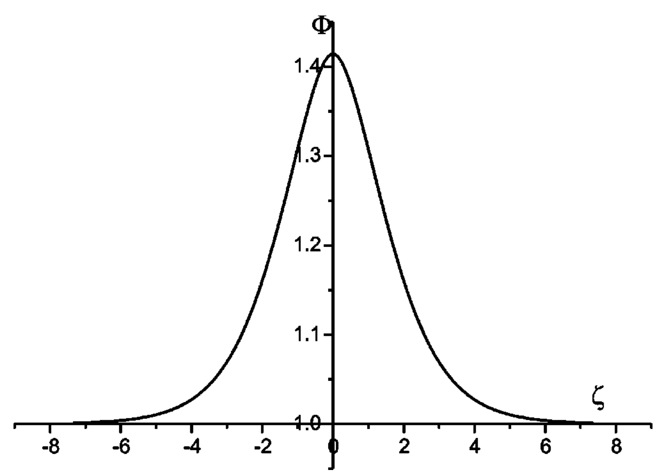

FIG. 11. Structure that resembles the form of a peakon, and emerges when the relations (i) are satisfied.

$$\sqrt{A}\zeta_{+++} \quad \text{if} \quad \sqrt{A}\zeta\in(-\infty,0] \quad \text{and} \quad -\sqrt{A}\zeta_{-+-} \quad \text{if} \quad \sqrt{A}\zeta\in[0,\infty) \quad \text{(a)},$$

$$\sqrt{A}\zeta_{+++} \quad \text{if} \quad \sqrt{A}\zeta\in\left(-\infty,\frac{\pi}{2}\right] \quad \text{and} \quad -\sqrt{A}\zeta_{--+} \quad \text{if} \quad \sqrt{A}\zeta\in\left[\frac{\pi}{2},\infty\right) \quad \text{(b)}.$$

The corresponding pattern structures are represented in Figs. 3 (a) and 4 (b). These are kinklike solitons; the second one has a little peak near its center. They can be interpreted as domain wells traveling along the medium.

For

$$\Phi\to 1 \quad \text{while} \quad \zeta\to-\infty \quad \text{and} \quad \Phi\to 1 \quad \text{while} \quad \zeta\to\infty \tag{18}$$

the solutions are determined by

$$\sqrt{A}\zeta_{-+-} \quad \text{if} \quad \sqrt{A}\zeta\in(-\infty,0] \quad \text{and} \quad -\sqrt{A}\zeta_{-+-} \quad \text{if} \quad \sqrt{A}\zeta\in[0,\infty) \quad \text{(c)},$$

$$\sqrt{A}\zeta_{++-} \quad \text{if} \quad \sqrt{A}\zeta\in(-\infty,0] \quad \text{and} \quad -\sqrt{A}\zeta_{++-} \quad \text{if} \quad \sqrt{A}\zeta\in[0,\infty) \quad \text{(d)}.$$

These structures exist as excitations in the condensate state, like a rarefaction of the field. Their forms [see Figs. 5 (c) and 6 (d)] suggest the names peak bubble and cusp bubble, respectively. Additionally we have

$$\sqrt{A}\zeta_{--+} \quad \text{if} \quad \sqrt{A}\zeta\in\left(-\infty,-\frac{\pi}{2}\right] \quad \text{and} \quad -\sqrt{A}\zeta_{++-} \quad \text{if} \quad \sqrt{A}\zeta\in\left[-\frac{\pi}{2},\infty\right) \quad \text{(e)}.$$

This is the usual peak soliton (7) and exists as an excitation to the nonzero background (see Fig. 7).

For

$$\Phi\to -1 \quad \text{while} \quad \zeta\to-\infty \quad \text{and} \quad \Phi\to -1 \quad \text{while} \quad \zeta\to\infty, \tag{19}$$

the two branches

$$\sqrt{A}\zeta_{+++} \quad \text{if} \quad \sqrt{A}\zeta\in\left(-\infty,\frac{\pi}{2}\right] \quad \text{and} \quad -\sqrt{A}\zeta_{-++} \quad \text{if} \quad \sqrt{A}\zeta\in\left[-\frac{\pi}{2},\infty\right) \quad \text{(f)}$$

merge together and produce the configuration named the loop soliton (Fig. 8).

Let us now consider the case of solutions that are specially obtained by coalescing two branches of each solution pair in Eq. (15) for the second type of nonzero gap Δ_2 in Eq. (16).

For the boundary condition (17), the solutions are

$$\sqrt{A}\left(\zeta_{+--}+\frac{\pi}{2}\right) \quad \text{if} \quad \sqrt{A}\zeta\in(-\infty,0] \quad \text{and} \quad -\sqrt{A}\left(\zeta_{--+}-\frac{\pi}{2}\right) \quad \text{if} \quad \sqrt{A}\zeta\in[0,\infty) \quad \text{(g)},$$

$$\sqrt{A}\left(\zeta_{---}-\frac{\pi}{2}\right) \quad \text{if} \quad \sqrt{A}\zeta\in(-\infty,0] \quad \text{and} \quad -\sqrt{A}\left(\zeta_{+-+}+\frac{\pi}{2}\right) \quad \text{if} \quad \sqrt{A}\zeta\in[0,\infty) \quad \text{(h)}.$$

These relations, represented as pictures in Figs. 9 (g) and 10 (h) are usually referred to as shock waves because of the abrupt discontinuities that are observed when they are traveling. This suggests the interpretation of such solutions as propagating defects in the lattice. Shock waves are universal entities that are observed in many diverse nonlinear systems. However, it is surprising that they can appear analytically in the second order nonlinear equations (1).

For boundary conditions (18) the solutions can be constructed using the following two branches:

$$\sqrt{A}\left(\zeta_{++-}-\frac{\pi}{2}\right) \quad \text{if} \quad \sqrt{A}\zeta\in(-\infty,0] \quad \text{and} \quad -\sqrt{A}\left(\zeta_{++-}-\frac{\pi}{2}\right) \quad \text{if} \quad \sqrt{A}\zeta\in[0,\infty) \quad \text{(i)},$$

$$\sqrt{A}\left(\zeta_{--+}+\frac{\pi}{2}\right) \quad \text{if} \quad \sqrt{A}\zeta\in(-\infty,0] \quad \text{and} \quad -\sqrt{A}\left(\zeta_{--+}+\frac{\pi}{2}\right) \quad \text{if} \quad \sqrt{A}\zeta\in[0,\infty) \quad \text{(j)}.$$

Both solutions exist as excitations above the condensate state; the first one takes the form of a hump soliton [Fig. 11] while Fig. 12 (j) represents a peakon.

For boundary condition (19) the soliton structures can be obtained by utilizing the following relations:

$$\sqrt{A}\left(\zeta_{-++}+\frac{\pi}{2}\right) \quad \text{if} \quad \sqrt{A}\zeta\in\left(-\infty,\frac{\pi}{2}\right] \quad \text{and} \quad -\sqrt{A}\left(\zeta_{-++}+\frac{\pi}{2}\right) \quad \text{if} \quad \sqrt{A}\zeta\in\left[-\frac{\pi}{2},\infty\right) \quad (\text{k}),$$

$$\sqrt{A}\left(\zeta_{+++}-\frac{\pi}{2}\right) \quad \text{if} \quad \sqrt{A}\zeta\in(-\infty,0] \quad \text{and} \quad -\sqrt{A}\left(\zeta_{+++}-\frac{\pi}{2}\right) \quad \text{if} \quad \sqrt{A}\zeta\in[0,\infty) \quad (\text{l}).$$

The first pair is a loop soliton (see Fig. 13) and the second is another representative of the peakon (see Fig. 14).

All of these rich structures are obtained by considering the anharmonicity in the intersite interaction potential. In addition to the well-known solitons, different solitonic structures such as defectons, shocks, peakons, cusps, etc., can appear by fixing boundary conditions of condensed type. Looplike solitons similar to that found in [17] can also exist. Also, as one can observe from the solutions above reported, we have a peak bubble that exists as a rarefaction in the constant background field. Such structures were also obtained recently in other types of nonlinear differential equation, for example, in the coupled Dym equations by using the algebraic geometric approach [18]. Similar humps as nonlinear excitations to the ground state of condensate type have also recently been shown in plasma physics [19].

Below we calculate the energy of each structure that is shown above. Despite the very interesting shape that loop solitons possess, their energies show divergent values. This means that for real production of such structures we need infinite energy, and that is in accordance with the statements of the general theory of topological solitons. The twist needed to form loops can absorb infinite energy in one dimensional space if we have already fixed beforehand the conditions at infinity.

Let us now present the results for energies that can be obtained from

$$E_{total}=\int_{-\pi/2\gamma}^{\pi/2\gamma}\left[\frac{1}{2}\Phi_t^2+\frac{1}{2}C_l\Phi_x^2+\frac{1}{4}C_{nl}\Phi_x^4+\frac{1}{2}V_0(1-\Phi^2)^2\right]dx. \tag{20}$$

The final forms of the energies of all the structures found above are represented by the following expressions:

$$\frac{1}{8}\pi(u^2+C_l)\left(\frac{1}{A}\right)^{1/2}+\frac{3}{64}(\pi-2)C_{nl}\left(\frac{1}{A}\right)^{3/2}+\frac{1}{8}(6+\pi)\sqrt{A}V_0 \quad (\text{a}) \text{ and } (\text{c}), \tag{21}$$

$$\frac{1}{2}\left(\frac{2}{8}\pi+1\right)(u^2+C_l)\left(\frac{1}{A}\right)^{1/2}+\frac{1}{32}\left[5+\frac{3}{2}\pi\right]C_{nl}a\left(\frac{1}{A}\right)^{3/2}+\frac{1}{4}\left(\frac{1}{2}\pi+3\right)\sqrt{A}V_0 \quad (\text{b}),$$

$$\frac{E^i_{total}}{2}+\frac{E^j_{total}}{2} \quad (\text{e}),$$

$$\left(\frac{1}{2}-\frac{1}{8}\pi\right)(v^2+C_l)\left(\frac{1}{A}\right)^{1/2}+\frac{1}{16}\left[\frac{5}{2}-\frac{3}{4}\pi\right]C_{nl}a\left(\frac{1}{A}\right)^{3/2}+\left(-\frac{1}{8}\pi+\frac{3}{4}\right)a\sqrt{A}V_0 \quad (\text{g}) \text{ and } (\text{j}),$$

$$\left(\frac{1}{8}\pi-\frac{1}{2}\ln 2\right)(v^2+C_l)\left(\frac{1}{A}\right)^{1/2}+\frac{1}{16}\left[\frac{33}{16}-\frac{21}{32}\pi\right]C_{nl}a\left(\frac{1}{A}\right)^{3/2}+\left(\frac{3}{4}+\frac{1}{8}\pi\right)a\sqrt{A}V_0 \quad (\text{h}) \text{ and } (\text{i}),$$

$$\left(\frac{3}{8}\pi+\frac{1}{2}\right)(v^2+C_l)\left(\frac{1}{A}\right)^{1/2}+\frac{1}{16}\left[\frac{5}{2}+\frac{9}{4}\pi\right]C_{nl}a\left(\frac{1}{A}\right)^{3/2}+\left(\frac{3}{8}\pi+\frac{3}{4}\right)a\sqrt{A}V_0(\text{l}).$$

For (d), (f), and (k), the total energy diverges. The energies of all our soliton structures are restricted by their velocities. Thus to avoid singularities in energy values, from Eq. (21) it is necessary to impose the condition

$$A=\frac{4V_0}{u^2-C_l}>0. \tag{22}$$

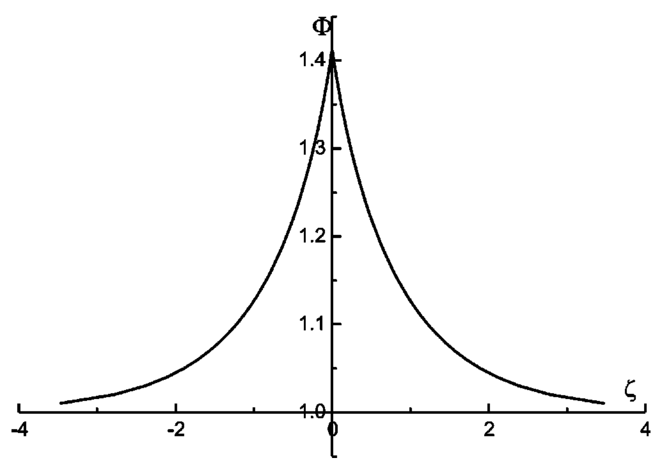

FIG. 12. Plot showing the form of a peakon obtained by merging two branches as is explained in the relations (j).

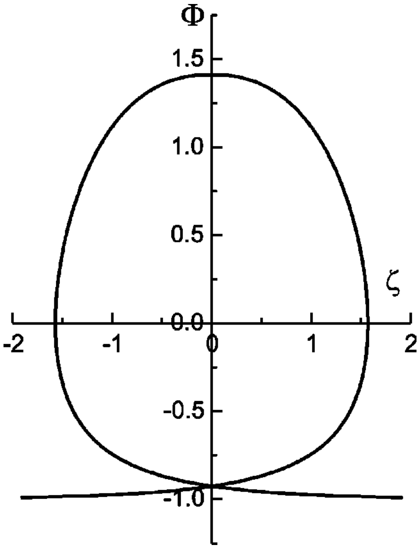

FIG. 13. Representation of an exotic loop soliton for the expressions (k). After evaluation of the energy of this configuration one finds that it diverges.

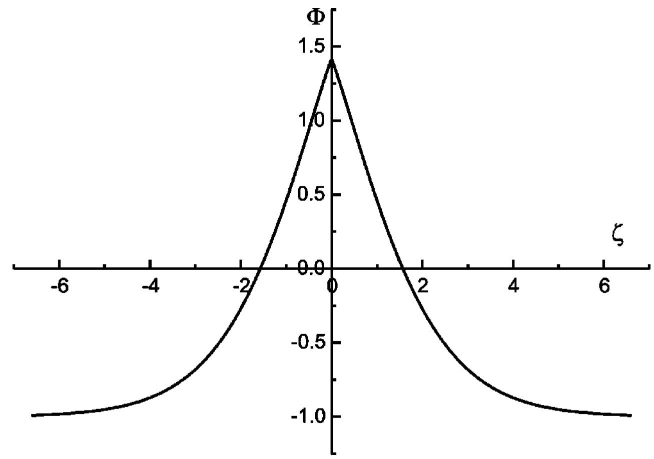

FIG. 14. We can observe here the plot of a typical peak soliton for the structure (l) in text.

III. PROPERTIES OF THE SOLITON SOLUTIONS

A small deviation from the vacuum solutions $\Phi=\Phi_0+\eta,|\eta|\ll 1$, for solutions with trivial $\Phi_0=0$ and condensed vacuum $\Phi_0=1$ is described by the linearized equation

$$\eta_{tt}-C_l\eta_{xx}+\mu^2\eta=0 \tag{23}$$

with $\mu=-2V_0$ for solutions above the trivial vacuum and $\mu=4V_0$ for solutions with condensate boundary conditions. The solutions of Eq. (23) are plane traveling waves with dispersion

$$\omega^2=C_lk^2+\mu^2.$$

Consequently, the vacuum will be stable if $k^2>-\mu^2/C_l$. Then the linear excitations above the trivial vacuum correspond to particles of mass $\mu=\sqrt{-2V_0}$, and $\mu=\sqrt{4V_0}$ for solutions with nontrivial vacua.

For the trivial boundary condition in the parameter space we obtained a restriction (6) under which drop compactons and peakons could exist. As was demonstrated above, the energy of these structures tends to be divergent as the velocity approaches the value of u_0.

From Eqs. (6) and (14) it is not difficult to derive the possible velocity values of drop compactons and peakons, $u=u_I$, and of the whole family of solutions with velocities $u=u_{II}$ with condensed boundary conditions. The explicit expression for the velocity u is presented as follows:

$$(u)^2=C_l\pm\sqrt{-6V_0C_{nl}}. \tag{24}$$

Thus we find a formal degeneracy of the velocity for solitonic structures satisfying the two different types of boundary condition at infinity. This apparent degeneracy disappears when the energy expressions for both types of solution [Eqs. (10), (11), and (21)] are analyzed. Indeed, studying the nonlinear excitation above the trivial vacuum, the drop compactons and peakons will travel with velocities with the sign + in the right hand side of Eq. (24) when

$$V_0>0,\quad u^2-C_l>0,\quad \text{and}\quad C_{nl}<0, \tag{25}$$

and with negative sign when

$$V_0<0,\quad u^2-C_l<0,\quad \text{and}\quad C_{nl}>0. \tag{26}$$

The solutions above a condensed vacuum possess completely inverse properties; for instance, the sign (+) in the right hand side of Eq. (24) will occur if $V_0<0$, $u^2-C_l>0$, and $C_{nl}>0$, and similarly for the negative sign. For both cases static configurations are available when $V_0=-(C_l)^2/6C_{nl}$. Finally, we can say that they exist in different sectors of the main parameters V_0 and C_{nl}.

For solutions satisfying condensate boundary conditions, the strong localizations are determined by the topological invariant charge associated with their field values at infinity. On the other hand, both parts of the coalescing solutions travel with equal velocity u in the same direction. All these requirements satisfy the restriction imposed on A in Eq. (22) to be positive. Additionally, if $u^2-C_l=0$ we should need infinite energy values because of Eqs. (10), (11), and (21). This situation can be avoided since it represents a nonphysical situation.

Next, we consider the scale transformation $\Phi_\alpha=\Phi(\alpha\zeta)$ for the solutions with trivial vacuum. The initial Hamiltonian for the stationary field $\Phi(\zeta)$ can be rewritten as

$$H=T_1+T_2+U_1, \tag{27}$$

with

$$T_1=\frac{1}{2}(u^2+C_l)\int(\Phi_\zeta)^2d\zeta,\quad T_2=\frac{1}{4}C_{nl}\int(\Phi_\zeta)^4d\zeta,$$

$$U_1=V_0\int(\Phi^2/2-1)\Phi^2d\zeta.$$

As is obvious, the extremum of the Hamiltonian (27) will be given by the solution Φ_α when $\alpha=1$ [20]. Under this transformation, Eq. (27) becomes

$$H[\Phi_\alpha]=\alpha T_1+\alpha^3 T_2+\frac{1}{\alpha}U_1. \tag{28}$$

Using $(dH/d\alpha)_{\alpha=1}$ we can get the virial relation

$$T_1+3T_2-U_1=0.$$

From Eq. (28) it also follows that for stable structures under these transformations (α oscillations) the second variation $\delta^2 H$ of the Hamiltonian (28) has to satisfy the following relation:

$$\left(\frac{d^2H}{d\alpha^2}\right)_{\alpha=1}=2(3T_2+U_1)>0. \tag{29}$$

First, by making use of the relation (10) for drop solutions, the second variation $\delta^2 H$ represented by Eq. (29) takes the form

$$\delta^2 H=-\frac{\pi V_0\sqrt{u^2-C_l}}{\sqrt{2}\sqrt{V_0}}. \tag{30}$$

In order to have positive values of $\delta^2 H$ we need

$$V_0<0 \quad \text{and} \quad u^2<C_l, \tag{31}$$

which correspond to solutions with velocity values [according to Eq. (26)]

$$(u)^2=C_l-\sqrt{-6V_0C_{nl}}. \tag{32}$$

For peakons, the same treatment gives us the restriction for finding stable solitons for which the second variation of the Hamiltonian gives

$$\delta^2 H=\frac{1}{2\sqrt{2}}\frac{(C_l-u^2)\sqrt{V_0}}{\sqrt{u^2-C_l}}. \tag{33}$$

For positivity of the second variation of the Hamiltonian (33) it is necessary to have once again the same restriction (31) as in the case of drop compactons. Consequently, these solutions will have the velocity values determined by Eq. (32). Then, the case of physical interest could occur when the restriction (31) is satisfied, meaning that, for this case, the solutions under consideration (peakons and drop compactons) are stable with respect to α oscillations.

Second, just as we did in our study of solutions with trivial boundary conditions, here we also use the α scale transformation and find the following condition of stability under this transformation for the whole class of energies displayed in Eq. (21). The second variation for the Hamiltonian of this class is the same as in Eq. (29), but now with

$$T_2=\frac{1}{4}C_{nl}\int(\Phi_\zeta)^4 d\zeta, \quad U_2=\frac{1}{2}V_0\int(1-\Phi^2)^2 d\zeta.$$

It is noticeable that the energy formulas for all solutions encountered above have the following typical form in terms of the three parameters u, C_l, and V_0 [see Eq. (21)]:

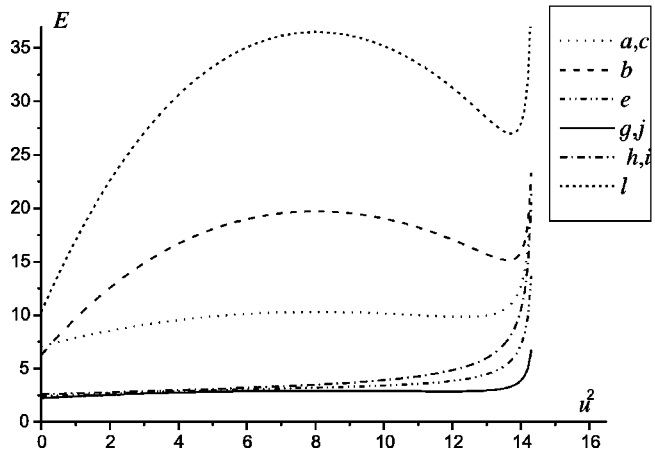

FIG. 15. Plot showing the dependence of the energy on the velocity for each structure with nontrivial vacuum at infinity. For the values $V_0=2, C_l=14.40$ the structures that resemble humps, defects, and peaks need less energy to be excited above their corresponding vacuum fields.

$$E=\alpha\frac{(u^2+C_l)\sqrt{C_l-u^2}}{2\sqrt{V_0}}-\beta\frac{(u^2-C_l)^2\sqrt{(C_l-u^2)^3}}{48V_0^2\sqrt{V_0}}+2\gamma V_0\sqrt{\frac{V_0}{C_l-u^2}},$$

α, β, and γ being the respective numerical coefficients of each term of the energy expression. In order to explore the stability of these structures under α oscillations we utilize Eq. (29) and after some calculation find that the structures with nontrivial vacuum can exhibit stability under α oscillations for

$$C_l>u^2>C_l-\kappa V_0 \tag{34}$$

when $V_0>0$, $C_l-u^2>0$, and $\kappa=2(2\gamma/\beta)^{1/4}$, or for

$$C_l+\kappa V_1>u^2>C_l \tag{35}$$

when $V_0=-V_1<0$, $C_l-u^2<0$, and $V_1>0$.

Next we turn to a qualitative explanation of which structures of all those presented here with the nontrivial vacuum are lowest in energy. To do this, we check how the energy depends on the velocity of each structure. In Fig. 15 we present the plots of this dependence. The structures with higher probability of appearing in this model are those that carry less energy in comparison with others for a given velocity. As we see from Fig. 15, these structures are those termed hump [(e) and (i)] and peak (j) solitons as different excitations to a constant field $\Phi=1$ When at infinity we have different field values $\Phi=\pm 1$, the shocklike structures (g) and (h) are those with more probability of appearing in comparison with the kinks, for example. These structures need less energy to become nonlinear excitations with respect to a constant field in the first case and to different constant field values in the second case.

For structures that emerge as nonlinear excitations above the trivial vacuum, the peakons are those that carry less energy in comparison to drop compactons for a given velocity. It is not difficult to check this statement by simply analyzing the analytic formulas for their energy.

Physically, these results are quite interesting, given the different applications that they could have in hydrodynamics, for instance: above the unperturbed constant surface of matter, under different perturbations, the interaction of nonlinearity and anharmonicity could lead to generation of peakons and bell-like structures, such as one can observe in a basin of liquid, for example.

Let us finally remark that, as was reported in [13] the kink compactons are available when $C_{nl}>0$. Our compacton solutions according to Eq. (26) also appear when this inequality is satisfied. In other words, this region of existence also shares the drop compactons obtained here with the sign $(-)$ in the right hand side of Eq. (24). This interesting behavior is very similar to that obtained in other reports in the literature. For instance, the drop solutions can coexist with kink solitons in the same parameter region of the cubic-quintic nonlinear Schrödinger equation [9]. They exist in the same region of the (one) parameter domain but in different vacuums. This feature seems at first glance to be universal, i.e., the coexistence in the parametric domain of drop solitons with kink solitons must be possible in many nonlinear systems.

IV. CONCLUSIONS

As is well known, the existence of solitons, and especially particular versions such as compactonlike structures in nonlinear equations (differential and discrete or integro-differential) implies strict requirements to be satisfied. Since solitonlike structures are very special solutions, in this paper we have obtained conditions determined by combinations of the parameters of the model in order to integrate the corresponding nonlinear evolution equations. We have demonstrated that anharmonicity in the interparticle interactions can allow the appearance of a rich variety of static and traveling solitonic structures. The configurations obtained here are determined specifically by applying two types of boundary condition, trivial and condensate, and by considering the sign of the coupling in the anharmonicity term of the intersite potential that provides additional attractive or repulsive interaction between sites. The trivial boundary condition allows the appearance of drop compacton and peak solitons, when the parameters satisfy the specific algebraic equations (6). When the boundary condition is of the condensate type and the relevant parameters satisfy Eq. (14), solitonic structures like defects, kinks, bubbles, peakons, and cusps were found. These solutions complement the rich family of solitonic structures already reported in the literature. At the same time, all structures will travel with the same velocity if we fix the parameters and the boundary conditions beforehand. It should be noted that the real values of the energies [Eqs. (10), (11), and (21)] of both types of solutions limit the values of the traveling velocity. For the appearance in the medium of exotic loop soliton structures, infinite energies are required. In the case of the condensed type of boundary condition, of all the variety of structures found here, the most probable to exist are structures like hump and peak solitons as nonlinear excitations above a constant field, while defects are of lower energy when the field has different vacuums at infinity. For solutions with the trivial vacuum, those termed peakons carry less energy for given velocity values. Using the virial approximation we can predict the region of validity for the velocities of all these structures and subsequently the conditions for their stability under the so-called α oscillations.

Checking the formulas for the velocities of both of these types of structure, one can easily find that there is a critical value of velocity that divides the regions of existence in the parameter space for both types of solution. This value corresponds to those structures found by Remoissenet and coworkers in [13–15]. For our solutions, this velocity value $u=\pm\sqrt{C_l}$ is inaccessible. Finally, we can say that much work must be done in the near future to relate these results to practical applications in nonlinear optics, for example, and to study the interactions between these solutions.

ACKNOWLEDGMENTS

The authors are indebted to Professor V. G. Makhankov for constant support and discussions. This work was supported in part by CONACYT-MEX Project No. 33147-E and UAEM Project No. 1420/2000.

[1] A. R. Bishop and T. R. Lewis, J. Phys. C **12**, 3811 (1979).
[2] J. A. Wattis, J. Phys. A **31**, 3301 (1998).
[3] M. Peyrard and M. D. Kruskal, Physica D **14**, 88 (1984).
[4] J. M. Speight and R. S. Ward, Nonlinearity **7**, 475 (1994).
[5] F. Zhang, Phys. Rev. E **54**, 4325 (1996).
[6] S. F. Flach, Y. Zolotaryuk and K. Kladko, e-print Patt-Sol/9812004.
[7] Y. S. Kivshar, Phys. Rev. E **48**, R43 (1993).
[8] J. Kaup, Physica D **25**, 361 (1987).
[9] V. G. Makhankov, *Soliton Phenomenology* (Kluwer Academic, Dordrecht, 1990).
[10] M. A. Agüero, Rev. Mex. Fis. **44**, 82 (1998).
[11] M. Agüero and R. Alvarado, Phys. Scr. **62**, 232 (2000).
[12] P. Rosenau and J. M. Hyman, Phys. Rev. Lett. **70**, 564 (1993).
[13] S. Dusuel, P. Michaux, and M. Remoissenet, Phys. Rev. E **57**, 2320 (1998).
[14] P. Tchofo Dinda and M. Remoissenet, Phys. Rev. E **60**, 6218 (1999).
[15] P. Tchofo Dinda, T. C. Kofane, and M. Remoissenet, Phys. Rev. E **60**, 7525 (1999).
[16] R. Camassa and D. D. Holm, Phys. Rev. Lett. **71**, 1661 (1993).
[17] A. J. Morrison, E. J. Parkes, and V. O. Vakhnenko, Nonlinearity **12**, 1427 (1999).
[18] M. S. Alber, G. G. Luther, and C. A. Miller, J. Math. Phys. **41**, 284 (2000).
[19] Chen Yinhua, Lei Wei, and M. Yu, Phys. Rev. E **61**, 809 (2000).
[20] V. G. Makhankov, Phys. Rep. **35**, 1 (1978).